Frontiers of Information Technology & Electronic Engineering
www.zju.edu.cn/jzus; engineering.cae.cn; www.springerlink.com
ISSN 2095-9184 (print); ISSN 2095-9230 (online)
E-mail: jzus@zju.edu.cn

# Using hybrid models to predict blood pressure reactivity to unsupported back based on anthropometric characteristics

Gurmanik KAUR‡, Ajat Shatru ARORA, Vijender Kumar JAIN

(*Sant Longowal Institute of Engineering and Technology, Deemed University, Punjab 148106, India*)

E-mail: mannsliet@gmail.com; ajatsliet@yahoo.com; vkjain27@yahoo.com

Received Aug. 18, 2014; Revision accepted Dec. 20, 2014; Crosschecked May 7, 2015

**Abstract:** Accurate blood pressure (BP) measurement is essential in epidemiological studies, screening programmes, and research studies as well as in clinical practice for the early detection and prevention of high BP-related risks such as coronary heart disease, stroke, and kidney failure. Posture of the participant plays a vital role in accurate measurement of BP. Guidelines on measurement of BP contain recommendations on the position of the back of the participants by advising that they should sit with supported back to avoid spuriously high readings. In this work, principal component analysis (PCA) is fused with forward stepwise regression (SWR), artificial neural network (ANN), adaptive neuro-fuzzy inference system (ANFIS), and the least squares support vector machine (LS-SVM) model for the prediction of BP reactivity to an unsupported back in normotensive and hypertensive participants. PCA is used to remove multi-collinearity among anthropometric predictor variables and to select a subset of components, termed 'principal components' (PCs), from the original dataset. The selected PCs are fed into the proposed models for modeling and testing. The evaluation of the performance of the constructed models, using appropriate statistical indices, shows clearly that a PCA-based LS-SVM (PCA-LS-SVM) model is a promising approach for the prediction of BP reactivity in comparison to others. This assessment demonstrates the importance and advantages posed by hybrid models for the prediction of variables in biomedical research studies.

**Key words:** Blood pressure (BP), Principal component analysis (PCA), Forward stepwise regression, Artificial neural network (ANN), Adaptive neuro-fuzzy inference system (ANFIS), Least squares support vector machine (LS-SVM)

**doi:**10.1631/FITEE.1400295 **Document code:** A **CLC number:** TP273; R544

## 1 Introduction

The error in arterial blood pressure (BP) measurement is influenced by many potential sources including faulty equipment, improper cuff size, white-coat effect, anxiety, caffeine intake, smoking shortly before BP monitoring, talking, noise, and body and arm postures of the participants (Pickering *et al.*, 2005). The unsupported back of the participant is responsible for a spurious overestimation of BP, termed 'BP reactivity to an unsupported back'. Studies have been reported that overestimation of BP may lead to inappropriate antihypertensive treatment, which exposes individuals unnecessarily to potential adverse side effects and increases health care cost (Chiatti *et al.*, 2012). Furthermore, inaccurate labeling leads to an increased perception of disease and absenteeism from work (Haynes *et al.*, 1978).

To our knowledge, there has been only one publication that investigated the effect of an unsupported back. Cushman *et al.* (1990) demonstrated a significant increase in diastolic BP (DBP) taken with the unsupported back in 48 hypertensive men.

Several epidemiological studies from different populations have reported significant correlation or multi-collinearity among anthropometric characteristics influencing BP (Baba *et al.*, 2007; de Hoog *et al.*, 2012; Kolade *et al.*, 2012; Moser *et al.*, 2013; Inoue

‡ Corresponding author
ORCID: Gurmanik KAUR, http://orcid.org/0000-0002-6384-4396

*et al.*, 2014), which leads to empirical under-identification of the BP prediction model (Smith and Sasaki, 1979). One of the approaches to eliminating the problem of multi-collinearity is principal component analysis (PCA). New variables obtained from PCA are uncorrelated. They can be used as input variables in subsequent analysis (Jolliffe, 2002).

In recent years, a variety of prediction models and their hybrids have been developed. Some of the recent research related to the prediction of BP by using traditional and soft computing models is discussed as follows: Monte-Moreno (2011) presented a system for simultaneous non-invasive estimate of the blood glucose level (BGL), systolic BP (SBP), and DBP using a photoplethysmograph (PPG) and machine learning techniques. Physiological properties including blood viscosity, vessel compliance, hemodynamics, metabolic syndrome, demographic characteristics, and emotional state were used as input variables. The machine learning techniques tested were as follows: ridge linear regression, multilayer perceptron artificial neural network (ANN), support vector machine (SVM), and random forest. The best results were obtained with the random forest technique. Genc (2011) proposed a linear stochastic model that integrates a known portion of the cardiovascular system and an unknown portion through parameter estimation to predict evolution of the mean arterial pressure (MAP). The performance of the model was tested in a case study from the clinical records in PhysioNet AHE (acute hypotensive episode) Challenge Training Data (http://www.physionet.org/challenge/2009/). They concluded that true positive rates (TPRs) and false positive rates (FPRs) were improved during the prediction period. Forouzanfar *et al.* (2011) presented a novel feature-based ANN for the estimate of BP from wrist oscillometric measurements. Unlike previous methods that use the raw oscillometric waveform envelope (OMWE) as an input to ANN, they used features extracted from the envelope. OMWE was mathematically modeled as a sum of two Gaussian functions. The optimum parameters of the Gaussian functions were found by minimizing the least squares error (LSE) between the model and OMWE using the Levenberg-Marquardt algorithm, and used as input features (Hagan and Menhaj, 1994). The performance of ANN was compared with that of the conventional maximum amplitude algorithm (MAA), adaptive neuro-fuzzy inference system (ANFIS), and already published ANN-based methods. It was found that the proposed approach achieves lower values of mean absolute error (MAE) and standard deviation of error (SDE) in the estimate of BP. Kurylyak *et al.* (2013) estimated the BP from the PPG signal using ANN. Training data were extracted from multi-parameter intelligent monitoring in an intensive care waveform database for better representation of possible pulse and pressure variation. The comparison between estimated and reference values showed better accuracy than the linear regression method. Golino *et al.* (2014) compared the classification tree technique with traditional logistic regression for the prediction of BP. Body mass index (BMI), waist circumference (WC), hip circumference (HC), and waist hip ratio (WHR) were used as predictor variables. Finally, the comparison of the classification tree technique with traditional logistic regression indicated that the former outperforms the latter in terms of predictive power. Huang *et al.* (2014) compared logistic regression, SVM, and the permanental classification method in predicting hypertension using genotype information. They used logistic regression analysis in the first step to detect significant single-nucleotide polymorphisms (SNPs). In the second step, they used the significant SNPs with logistic regression, SVM, and the permanental classification method for prediction purposes. The results showed that SVM and permanental classification both outperformed logistic regression. Khan *et al.* (2014) proposed SVM for performing the prediction of BP with primary emotions using Facebook status. Current human BP and those belonging to up to six previous primary emotions were given as input variables. The outcome showed that SVM can be prosperously applied for the prediction of BP through primary emotions. On the contrary, validations signified that the error statistics of the SVM model with the radial basis function (RBF) outperformed the SVM with the polynomial kernel function. Barbé *et al.* (2014) developed a logistic regression model to calibrate and correct an oscillometric monitor such that the device better corresponds to the Korotkoff method regardless of the health status of the patient. The model eliminates the systematic errors caused by patients suffering from hyper- or hypotension. They reported that the systematic error was reduced by

nearly 50% corresponding to the performance specifications of the device.

The aim of this research was to develop PCA-based forward stepwise regression (PCA-SWR), PCA-based ANN (PCA-ANN), PCA-based ANFIS (PCA-ANFIS), and PCA-based least squares support vector machine (PCA-LS-SVM) models for the prediction of BP reactivity to an unsupported back, based on anthropometric predictor variables including age, height, weight, BMI, and arm circumference (AC) in normotensive and hypertensive participants. The prediction performance of the developed models was assessed using the coefficient of determination ($R^2$), root mean square error (RMSE), and mean absolute percentage error (MAPE).

## 2 Data collection

A total of 40 normotensive and 30 hypertensive participants among students, staff, and faculty of Sant Longowal Institute of Engineering and Technology, Deemed University, India, volunteered for this study. The institutional research committee approved the research protocol and all participants gave written consent before participation.

A standard questionnaire was administrated to collect information on anthropometric characteristics of the participants. The study was conducted in a separate room to ensure minimal interference within the room while the tests were being carried out. The observers involved in this study were trained according to the BP measurement protocol of the British Hypertension Society (1998).

To eliminate observer bias, we measured BP using a validated, newly purchased, and fully automated sphygmomanometer OMRON HEM-7203 (OMRON Healthcare Co., Ltd., Japan), which uses the oscillometric method for measurement. The BP monitor was available with a small cuff (17–22 cm), medium cuff (22–32 cm), and large cuff (32–42 cm). The appropriate size of the cuff was determined from the mid-AC of the participants. The participants were instructed to empty their bladder prior to measurements. They were asked to sit upright with elbows on table, legs uncrossed, and feet flat on the ground, as these are the potential confounding factors. Moreover, they were asked not to talk or move during measurement (Pickering *et al.*, 2005). They were advised to avoid alcohol, smoking, coffee/tea, and exercise for at least 30 min before their BP measurement.

Before measuring BP the participants were made to rest for 5 min on a chair with supported back to allay anxiety. The measurements were performed four times repeatedly at an interval of 1 min by the same researcher from 9 to 12 noon. The first measurement was discarded and the average of the last three measurements was taken into account. Subsequently, the same measurement protocol was repeated with unsupported back when seated on the examination table. All measurements were obtained under similar conditions except for the different back positions (Cushman *et al.*, 1990). The participants were examined daily for seven days and the average BP was considered for further evaluation.

## 3 Experimental methods

### 3.1 Principal component analysis

Before applying PCA, Bartlett's test of sphericity (Tobias and Carlson, 1969) and the Kaiser-Meyer-Olkin (KMO) measure of sampling adequacy (Williams *et al.*, 2010) are used to check the suitability of data for the application of PCA.

Bartlett's test of sphericity is used to test the null hypothesis that the correlation matrix is an identity matrix, i.e.,

$$\chi^2 = -\left(N - 1 - \frac{2K+5}{6}\right)\ln|\boldsymbol{R}|, \tag{1}$$

where $\chi^2$ is the chi-square, $N$ the sample size, $K$ the number of predictor variables, and $|\boldsymbol{R}|$ the determinant of the correlation matrix.

The KMO index is used to compare the magnitude of calculated correlation coefficients and partial correlation coefficients. The formula for KMO is given as follows:

$$\mathrm{KMO} = \frac{\sum\limits_{i\neq j}\sum r_{ij}^2}{\sum\limits_{i\neq j}\sum r_{ij}^2 + \sum\limits_{i\neq j}\alpha_{ij}^2}, \tag{2}$$

where $r_{ij}$ is the Pearson's correlation coefficient between variables $i$ and $j$ and $\alpha_{ij}$ the partial correlation

coefficient between variables $i$ and $j$. The KMO index ranges from 0 to 1, and it should be greater than 0.6 for the PCA to be considered appropriate.

PCA is a multivariate statistical technique used to eliminate the multi-collinearity problem between independent variables by transforming the variables into principal components (PCs), which are independent linear combinations of the independent variables, and retain the maximum possible variance of the initial dataset.

The basic equation of PCA in matrix notation is

$$\boldsymbol{Y}=\boldsymbol{W}\boldsymbol{X}, \tag{3}$$

where $\boldsymbol{X}$ is the matrix about $p$ independent variables and $\boldsymbol{W}$ is the matrix of weights, each entry ($w_{ij}$) of which represents the standardized weight of the corresponding independent variable in PCs.

Varimax rotation is applied to obtain values of rotated factor loadings. The loading demonstrates the contribution of each independent variable in a specific PC. Details for mastering the art of PCA are referred to Noori *et al.* (2010).

### 3.2 Stepwise regression

In SWR, predictor variables are introduced into the model in an order determined by the strength of their association with the response variable to maximize the $R^2$ of the response variable (Card *et al.*, 1988).

At each step of the algorithm, the probability ($p$) of an F-statistics is determined to test a model with or without a new predictor variable. The F-statistics is expressed as follows:

$$F=\frac{\mathrm{RSS}_0-\mathrm{RSS}_1}{\mathrm{RSS}_1/(n-k+1)}, \tag{4}$$

where $\mathrm{RSS}_0$ is the residual sum of squares of the original model without the new variables, $\mathrm{RSS}_1$ the residual sum of squares with the new variables included, $k$ the number of variables present in the model, and $n$ the number of samples.

If a predictor variable is not included in the existing model, then the null hypothesis becomes that the predictor variable will have a zero coefficient if added to the model. The predictor variable can be added to the model if sufficient evidence can be found to reject the null hypothesis (Lynn *et al.*, 2009).

### 3.3 Artificial neural network

ANN is a computational model whose structure and function mimic the biological neural network of the human brain. It consists of a number of independent computational units, called neurons. The neurons communicate with each other through synaptic weights (Nauck, 1997).

Among all the paradigms of ANN, feed-forward (FF) is considered to be the best choice for this work. In an FF paradigm, the neurons in a layer receive weighted outputs from all neurons in the preceding layer and transmit their outputs to the next layer. Thus, all links between neurons are unidirectional and data are fed forward. The network is trained using an error back propagation training algorithm. It propagates the error (difference between the predicted and actual outputs) backward through the hidden layer to the input layer to iteratively adjust weights and biases to minimize the prediction error. Details have been described by Basheer and Hajmeer (2000).

Mathematically, the model can be expressed as

$$\boldsymbol{y}=f(\boldsymbol{x},\boldsymbol{\theta})+\boldsymbol{\varepsilon}, \tag{5}$$

where $\boldsymbol{x}$ is the vector of independent predictor variables, $\boldsymbol{\theta}$ the vector of weights, and $\boldsymbol{\varepsilon}$ a random error component. Or,

$$\boldsymbol{y}=f\left(v_{\mathrm{o}}+\sum_{j=1}^{m}h\left(\lambda_j+\sum_{i=1}^{n}\boldsymbol{x}_i w_{ij}\right)v_j\right), \tag{6}$$

where $v_{\mathrm{o}}$ is the output bias, $h(\cdot)$ is the hidden layer activation function, $n$ is the number of input units, $m$ is the number of hidden units, $\lambda_j$ ($j$=1, 2, …, $m$) is the bias of hidden unit, $\boldsymbol{x}_i$ ($i$=1, 2, …, $n$) is the input vector, $w_{ij}$ is the weight from input unit $i$ to hidden unit $j$, and $v_j$ is the weight from hidden unit $j$ to the output.

### 3.4 Adaptive neuro-fuzzy inference system

ANFIS is a multilayer FF network that employs the ANN learning algorithm and fuzzy reasoning to correctly associate the input values with the output values.

Suppose ANFIS has two inputs, $\boldsymbol{x}$ and $\boldsymbol{y}$, and an output $\boldsymbol{f}$. For a first-order Sugeno fuzzy model, a

common rule set with two fuzzy if-then rules, the rules can be written as follows:

Rule 1: if $\boldsymbol{x}$ is $A_1$ and $\boldsymbol{y}$ is $B_1$, then $\boldsymbol{f}_1=p_1\boldsymbol{x}+q_1\boldsymbol{y}+\boldsymbol{r}_1$, (7)

Rule 2: if $\boldsymbol{x}$ is $A_2$ and $\boldsymbol{y}$ is $B_2$, then $\boldsymbol{f}_2=p_2\boldsymbol{x}+q_2\boldsymbol{y}+\boldsymbol{r}_2$, (8)

where $A_1$, $A_2$ and $B_1$, $B_2$ are membership functions (MFs) for inputs $\boldsymbol{x}$ and $\boldsymbol{y}$ respectively, and $p_i$, $q_i$, and $\boldsymbol{r}_i$ ($i$=1, 2) are the linear parameters of the first-order Sugeno fuzzy model.

The proposed ANFIS model is a multilayer network consisting of five layers. The first layer consists of input adaptive nodes and represents the training values. The second layer consists of fixed nodes. The output of each node is the product of all the incoming signals and represents the firing strength of a rule. The third layer consists of fixed nodes. The $i$th node of this layer calculates the ratio of the $i$th rule's firing strength. The output is termed 'normalized firing strength'. The fourth layer consists of adaptive nodes. Parameters of this layer are known as consequent parameters. The fifth layer consists of a single output node, which computes the overall output as the summation of all incoming signals (Jang, 1993).

### 3.5 Least squares support vector machine

LS-SVM, a modified version of standard SVM, considers equality type of constraints instead of inequalities as in the standard SVM approach. This leads to solving a set of linear equations instead of a quadratic programming (QP) problem. Thus, LS-SVM reduces the computational complexity.

Consider a set of $N$ data points $\{\boldsymbol{x}_1, y_1, \boldsymbol{x}_2, y_2, \ldots, \boldsymbol{x}_N, y_N\}$, where $\boldsymbol{x}_i\in\mathbb{R}^N$ is the $i$th input vector and $y_i\in\mathbb{R}$ is the corresponding output. In the feature space, LS-SVM can be described as

$$\boldsymbol{y}(\boldsymbol{x})=\boldsymbol{w}^{\mathrm{T}}\boldsymbol{\Phi}(\boldsymbol{x})+\boldsymbol{b}, \tag{9}$$

where $\boldsymbol{\Phi}(\boldsymbol{x})$ is a non-linear function that maps the input data into a higher dimensional feature space, $\boldsymbol{w}$ the weight vector, and $\boldsymbol{b}$ the bias term.

The constrained optimization problem of LS-SVM is to minimize a cost function $C$ containing a penalized regression error ($\boldsymbol{e}$):

$$\min C(\boldsymbol{w}, \boldsymbol{e})=\frac{1}{2}\boldsymbol{w}^{\mathrm{T}}\boldsymbol{w}+\frac{1}{2}\gamma\sum_{i=1}^{N}\boldsymbol{e}_i^2 \tag{10}$$

subject to the following equality constraint:

$$\boldsymbol{y}=\boldsymbol{w}^{\mathrm{T}}\boldsymbol{\Phi}(\boldsymbol{x}_i)+\boldsymbol{b}+\boldsymbol{e}_i, \tag{11}$$

where $\boldsymbol{e}_i$ is the error vector ($i$=1, 2, …, $N$) and $\gamma$ is the regularization parameter.

Solving the above optimization problem in dual space leads to finding the coefficients $\alpha_i$ and $\boldsymbol{b}$ in the following solution:

$$\boldsymbol{y}(\boldsymbol{x})=\sum_{i=1}^{N}\alpha_i K(\boldsymbol{x}, \boldsymbol{x}_i)+\boldsymbol{b}, \tag{12}$$

where $K(\boldsymbol{x}, \boldsymbol{x}_i)$ is the kernel function defined as the dot product between $\boldsymbol{\Phi}(\boldsymbol{x})$ and $\boldsymbol{\Phi}(\boldsymbol{x}_i)$.

Using the kernel function to replace the inner product of Eq. (12), we can realize non-linear regression, which can effectively overcome the dimension disasters and local optimal problems. Commonly used kernel functions are polynomial, Gaussian, linear, sigmoid, and radial basis functions (Suykens and Vandewalle, 1999).

## 4 Results

Descriptive statistics for each anthropometric characteristic are given as mean and standard deviation (SD) (Table 1).

### 4.1 Effect of unsupported back on blood pressure

The results of a paired $t$-test demonstrated that there is no statistically significant difference between

**Table 1 Anthropometric characteristics of study samples**

| Anthropometric characteristic | Mean | | SD | |
|---|---|---|---|---|
| | Normotensive | Hypertensive | Normotensive | Hypertensive |
| Age (year) | 23.10 | 42.83 | 1.24 | 6.67 |
| Height (m) | 1.61 | 1.58 | 0.03 | 0.04 |
| Weight (kg) | 55.96 | 62.48 | 7.29 | 10.89 |
| BMI (kg/m$^2$) | 21.55 | 23.57 | 2.50 | 3.49 |
| AC (cm) | 26.56 | 26.73 | 2.45 | 2.40 |

BMI: body mass index; AC: arm circumference

SBP measurements of a supported and an unsupported back ($p$=0.0759 for normotensive participants and 0.1157 for hypertensive participants). However, we found a significantly higher DBP, $p$<0.001, in all participants (Table 2). These results are consistent with the recommendations of the American Heart Association (AHA) Council for BP measurement in humans and experimental animals (Pickering *et al.*, 2005).

### 4.2 Multi-collinearity diagnostic

A visual inspection of Pearson's correlation coefficients (Table 3) revealed an intense correlation or the existence of multi-collinearity (correlation coefficient>0.6) between pairs of anthropometric characteristics (Gujarati, 1995) in all participants. PCA omits the multi-collinearity between anthropometric characteristics and simplifies the complexity of the relationship between them (Jolliffe, 2002).

### 4.3 Principal component analysis of blood pressure data

Firstly, Bartlett's sphericity test was applied to verify the applicability of PCA. The value of $\chi^2$ was 231.012 (normotensive participants) and 119.480 (hypertensive participants) with a degree of freedom of 10 and $p$<0.0001. A high value of $\chi^2$ implied that PCA is applicable to our dataset. The overall KMO index was computed as 0.63 for normotensive and 0.75 for hypertensive participants, which indicates that the sample size is enough to apply PCA (Kaiser, 1960). Out of five PCs, only the first four PCs (PC1–PC4), explaining more than 5% of total variation, were retained for further analysis. In normotensive participants, the selected PCs explained 99.8% of the total variation. Variance proportions explained by PC1, PC2, PC3, and PC4 were found as 71.84%, 16.58%, 6.34%, and 5.04%, respectively. In hypertensive participants, the selected PCs explained 98.04% of the total variation. Variance proportions accounted for by PC1, PC2, PC3, and PC4 were estimated to be 61.10%, 22.50%, 8.78%, and 5.66%, respectively. PCs may be interpreted from the anthropometric characteristics that are highly correlated with them. Loadings after varimax rotation give an indication of the extent to which the original variables are influential in forming new variables (Sharma, 1995). The loadings of anthropometric characteristics in selected PCs are shown in Table 4. For both normotensive and hypertensive participants, weight and BMI were the characteristics having the highest correlation with PC1 and height had the highest correlation with PC2. Moreover, Pearson's correlation between PCs as shown in Table 5 indicates that the problem of multi-collinearity presented in Table 3 was solved. There are no significant relationships between any pair of PCs in the correlation table (correlation coefficient<0.6).

To develop PCA-based prediction models, principal scores obtained from the principal score coefficients were used as independent variables and BP reactivity to an unsupported back was used as a dependent variable. Moreover, 80% of data were used

**Table 3 Pearson's correlation coefficients between pairs of anthropometric characteristics in normotensive and hypertensive participants**

| Variable | Height (m) | Weight (kg) | BMI (kg/m$^2$) | AC (cm) |
|---|---|---|---|---|
| Age (year) | 0.535 (0.113) | 0.784* (0.598) | 0.701* (0.509) | 0.668* (0.585) |
| Height (m) | | 0.543 (0.165) | 0.237 (0.305) | 0.619* (0.021) |
| Weight (kg) | | | 0.934* (0.885*) | 0.743* (0.767*) |
| BMI (kg/m$^2$) | | | | 0.617* (0.691*) |

BMI: body mass index. * $p$<0.001. Values in brackets indicate correlations in anthropometric characteristics of hypertensive participants

**Table 2 Results of paired *t*-test**

| Type of participants | BP | Difference (mean±SD) | $t$ | $p$ | 95% CI of mean difference |
|---|---|---|---|---|---|
| Normotensive | SBP | 0.0073±0.0254 | 1.8236 | 0.076 | −0.0008–0.0154 |
| | DBP | 4.5357±2.3045 | 12.4482 | <0.001 | 3.7987–5.2727 |
| Hypertensive | SBP | 0.0107±0.0360 | 1.6216 | 0.116 | −0.0028–0.0241 |
| | DBP | 7.2460±1.9886 | 19.9581 | <0.001 | 6.5035–7.9886 |

CI: confidence interval; SBP: systolic blood pressure; DBP: diastolic blood pressure

**Table 4 Loadings after varimax rotation of anthropometric characteristics in normotensive and hypertensive participants**

| Anthropometric characteristics | PC1 | | PC2 | | PC3 | | PC4 | |
|---|---|---|---|---|---|---|---|---|
| | Normo. | Hyper. | Normo. | Hyper. | Normo. | Hyper. | Normo. | Hyper. |
| Age (year) | 0.0004 | −0.0036 | −0.0006 | 0.0020 | −0.0000 | **0.9988** | **−1.0000** | −0.0026 |
| Height (m) | −0.0139 | 0.0058 | **−0.9676** | **0.9968** | 0.0002 | 0.0020 | −0.0008 | 0.0043 |
| Weight (kg) | **−0.6569** | **0.6576** | −0.1812 | 0.0561 | −0.0008 | −0.0349 | 0.0039 | −0.0754 |
| BMI (kg/m$^2$) | **−0.7538** | **0.7533** | 0.1757 | −0.0566 | 0.0008 | 0.0352 | −0.0039 | 0.0760 |
| AC (cm) | −0.0001 | 0.0078 | 0.0001 | −0.0043 | **−1.0000** | 0.0027 | −0.0000 | **−0.9942** |

BMI: body mass index; AC: arm circumference. Normo.: normotensive; Hyper.: hypertensive. Bold values indicate the highest correlations between anthropometric characteristics and the corresponding components

**Table 5 Pearson's correlation coefficients among all pairs of PCs in normotensive and hypertensive participants**

| | PC2 | PC3 | PC4 |
|---|---|---|---|
| PC1 | $-2.25\times10^{-6}$ | $7.98\times10^{-8}$ | $-1.67\times10^{-5}$ |
| | ($8.78\times10^{-6}$) | ($4.23\times10^{-6}$) | ($6.59\times10^{-6}$) |
| PC2 | | $-7.237\times10^{-16}$ | $5.808\times10^{-16}$ |
| | | ($9.19\times10^{-6}$) | ($1.42\times10^{-5}$) |
| PC3 | | | $-7.557\times10^{-17}$ |
| | | | ($1.75\times10^{-5}$) |

Values in brackets indicate correlations in anthropometric characteristics of hypertensive participants

for training while the entire dataset was used for testing. MATLAB Version 7.5 was used to develop the prediction models.

### 4.4 Principal component analysis based forward stepwise regression

When probabilities were taken into consideration, the regression of standardized BP reactivity on PC3 (composed of AC) was found statistically significant in normotensive individuals. PC1 (composed of weight and BMI) and PC2 (composed of height) were found to be statistically significant in hypertensive individuals. The final model equation for normotensive participants is given as follows:

$$\text{DBP reactivity}=4.536+15.5933\times\text{PC3}. \quad (13)$$

The final model equation for hypertensive participants is given as follows:

$$\text{DBP reactivity}=8.579+1.3250\times\text{PC1}+1.0814\times\text{PC2}. \quad (14)$$

Figs. 1a and 1b show the scatter plots between observed and predicted values of BP reactivity from the PCA-SWR model in normotensive and hypertensive participants, respectively.

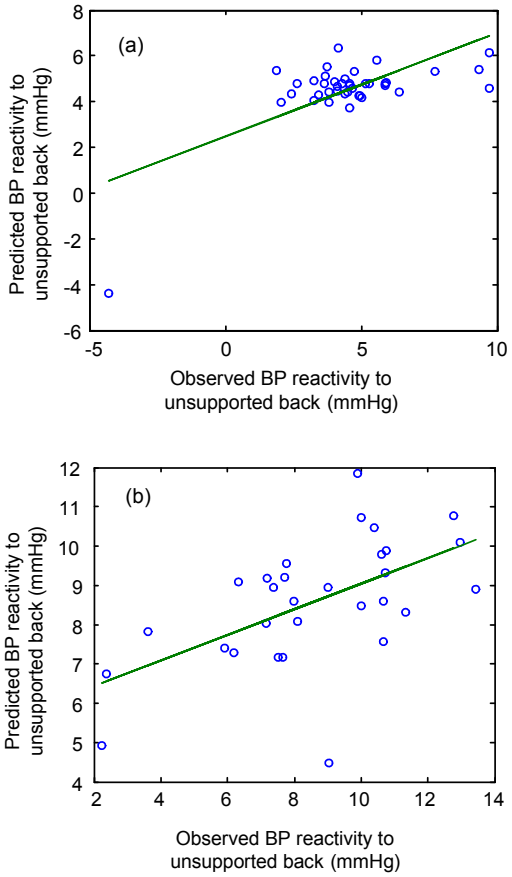


**Fig. 1 Scatter plots between observed and predicted values of DBP reactivity using the PCA-SWR model in normotensive (a) and hypertensive (b) participants, respectively**

### 4.5 Principal component analysis based artificial neural network

A PCA-ANN model with two hidden layers was also developed. As activation functions, tangent

sigmoid and linear transfer functions (TFs) were used in the hidden and output layers, respectively. The number of hidden nodes directly affects the performance of ANN. Thus, many experimental investigations were conducted to determine the optimal number of hidden nodes. There was one input layer with four input nodes (representing four PCs), two hidden layers with six hidden nodes in each layer, and one output layer with one output node (representing BP reactivity to an unsupported back). The back propagation learning algorithm based on the Levenberg-Marquardt technique was used to find the local minimum of the error function. It is more powerful and faster than the conventional gradient descent technique (Hagan and Menhaj, 1994).

The observed and predicted values of BP reactivity from the PCA-ANN model for normotensive and hypertensive participants are illustrated in Figs. 2a and 2b, respectively.

### 4.6 Principal component analysis based adaptive neuro-fuzzy inference system

A Sugeno-type fuzzy inference system was developed using 'genfis1' with grid partition on data. Different ANFIS parameters were tested to achieve the perfect training and the maximum prediction accuracy. Input MF 'gauss2mf' and 'pimf' were used in normotensive and hypertensive participants respectively and output MF 'linear' was used. Other parameters of the trained PCA-ANFIS model were: number of MFs=16, number of nodes=55, number of linear parameters=80, number of non-linear parameters=32, total number of parameters=112, and number of fuzzy rules=16.

The observed and predicted values of BP reactivity from the PCA-ANFIS model for normotensive and hypertensive participants are illustrated in Figs. 3a and 3b, respectively.

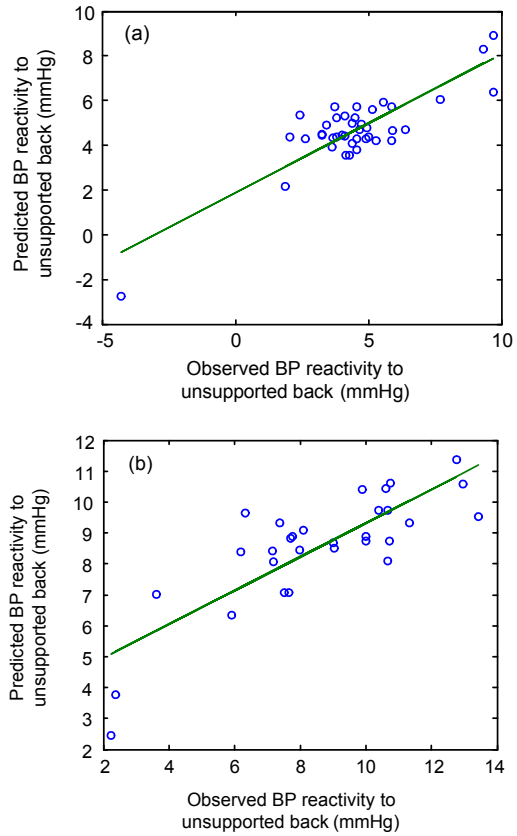


**Fig. 2 Scatter plots between observed and predicted values of DBP reactivity using the PCA-ANN model in normotensive (a) and hypertensive (b) participants, respectively**

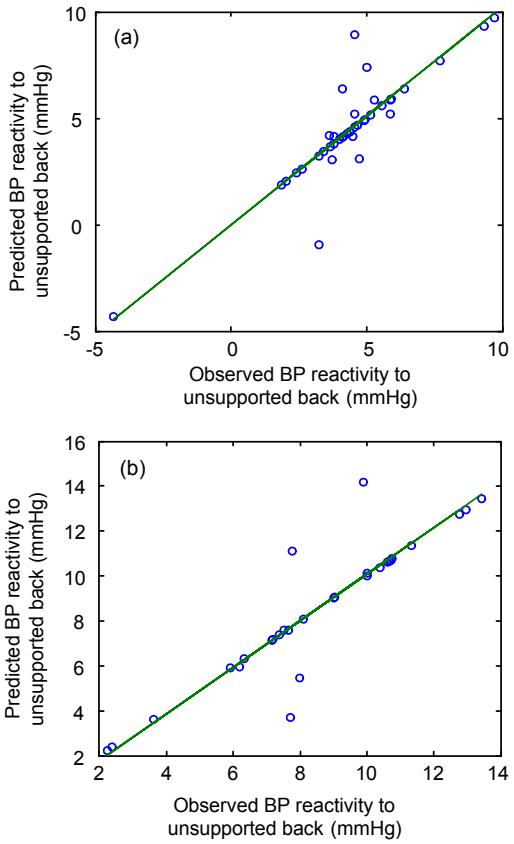


**Fig. 3 Scatter plots between observed and predicted values of DBP reactivity using the PCA-ANFIS model in normotensive (a) and hypertensive (b) participants, respectively**

### 4.7 Principal component analysis based least squares support vector machine

To develop a PCA-LS-SVM prediction model, the most important steps are kernel and parameter selection, because they can significantly affect the model performance; consequently, we used the RBF kernel and applied the grid search optimization algorithm with two-fold cross-validation to obtain the optimal parameter combination or minimum mean square error (MSE) (Schölkopf and Smola, 2002). The optimal values of regularization parameter ($\gamma$) and squared bandwidth ($\sigma^2$) in normotensive and hypertensive participants were $\gamma$=6.5343×10$^3$, $\sigma^2$=0.0929 and $\gamma$=5.1151×10$^4$, $\sigma^2$=0.0600, respectively.

Figs. 4a and 4b show the scatter plots between observed and predicted values of BP reactivity from the PCA-LS-SVM model in normotensive and hypertensive participants, respectively.

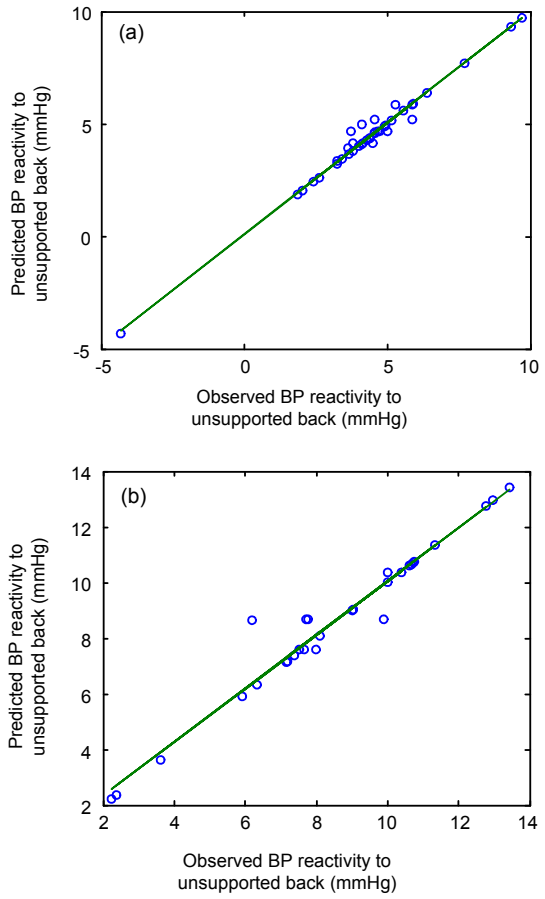


**Fig. 4 Scatter plots between observed and predicted values of DBP reactivity using the PCA-LS-SVM model in normotensive (a) and hypertensive (b) participants, respectively**

Comparisons of the statistical indices of the four models as shown in Table 6 revealed that the PCA-LS-SVM model has the highest value of $R^2$ and lowest value of RMSE and MAPE for prediction of BP reactivity to an unsupported back in normotensive participants.

## 5 Discussion

Accurate measurement of BP is critical for making appropriate diagnosis and management of hypertension because it is the leading preventable risk factor for premature deaths. An inaccurate measurement of BP could lead to a participant being falsely classified as having hypertension or normal BP, which leads to faulty clinical decisions (O'Brien *et al.*, 2003).

The rise in BP with unsupported back may be due to the isometric exercise of the back muscles which increases peripheral vascular resistance and DBP (Pickering *et al.*, 2005).

This study clearly demonstrates that the unsupported back in a sitting position significantly increases the DBP of normotensive and hypertensive participants. A similar conclusion was found by Cushman *et al.* (1990).

In addition, four hybrid models for prediction of BP reactivity to an unsupported back are put forward in this paper. According to our knowledge, there is no study including the same variables and prediction models as those in our study. Therefore, the results were compared with indirectly related studies (Table 7).

Higher performance of soft computing models in all studies was sourced from a greater degree of robustness and fault tolerance than that of traditional models. Specifically, in this study, the best performance was obtained with the PCA-LS-SVM model. Due to the use of statistical learning theory, LS-SVM has several advantages, i.e., a global optimal solution, fast convergence, and especially good generalization when only a few samples are available.

Our study has a number of advantages. We used small, medium, and large size cuffs, which may have produced more accurate readings. We took the mean of multiple measurements to enhance the

**Table 6 Statistical indices for different models**

| Model | $R^2$ (%) | | RMSE | | MAPE (%) | |
|---|---|---|---|---|---|---|
| | Normotensive | Hypertensive | Normotensive | Hypertensive | Normotensive | Hypertensive |
| PCA-SWR | 45.22 | 32.60 | 1.6842 | 2.3954 | 29.20 | 29.90 |
| PCA-ANN | 71.86 | 66.71 | 0.5421 | 0.5862 | 24.80 | 18.30 |
| PCA-ANFIS | 80.75 | 82.67 | 0.4954 | 0.4686 | 11.20 | 5.92 |
| PCA-LS-SVM | 98.49 | 95.95 | 0.1243 | 0.2013 | 3.01 | 2.90 |

$R^2$: coefficient of determination; RMSE: root mean square error; MAPE: mean absolute percentage error

**Table 7 Comparison of results with other studies**

| Study | Model developed | Predicted parameter | Remarks |
|---|---|---|---|
| Monte-Moreno, 2011 | Ridge linear regression, ANN, SVM, random forest | BGL, BP | Random forest technique outperformed ridge linear regression, ANN, and SVM. $R^2$=0.91 (SBP), $R^2$=0.89 (DBP), $R^2$=0.90 (BGL) |
| Genc, 2011 | Linear stochastic model | MAP | FPRs and TPRs were improved with an increased number of data points during the estimation period. The prediction onset time decreased for several records |
| Forouzanfar *et al.*, 2011 | ANN (raw-input), ANN (feature based), MAA, ANFIS (feature based) | SBP, DBP from wrist oscillometric measurements | ANN (feature based) achieved the best performance compared to other models. For SBP predictions: MAE=6.28, SDE=8.58. For DBP predictions: MAE=5.73, SDE=7.33 |
| Kurylyak *et al.*, 2013 | ANN | SBP, DBP | The experimental results confirmed the correctness of ANN when compared with the linear regression model. Mean±SD: 3.80±3.46 for SBP, 2.21±2.09 for DBP. Relative error: 3.48±3.19 for SBP, 3.90±3.51 for DBP |
| Golino *et al.*, 2014 | Classification tree, logistic regression | SBP, DBP | The classification tree technique outperformed the traditional logistic regression technique in terms of predictive power |
| Huang *et al.*, 2014 | Logistic regression, SVM, permanental classification method | SBP, DBP | The error rates were reduced from about 22% for multi-SNP logistic regression to 12% for SVM and permanental classification, when the most significant 100 SNPs from single-SNP logistic regression were used as predictors |
| Khan *et al.*, 2014 | SVM with RBF and polynomial kernel | SBP, DBP | SVM (RBF kernel) outperformed SVM (polynomial kernel). Coefficient of correlation $R$=0.97 (SBP), 0.96 (DBP). RMSE=6.94 (SBP), 5.78 (DBP). Scatter index (SI)=22.34 (SBP), 22.79 (DBP) |
| Barbé *et al.*, 2014 | Logistic ordinal regression | SBP, DBP | RMSE before calibration: 12.75 mmHg for SBP and 7.91 mmHg for DBP. RMSE after calibration: 6.02 mmHg for SBP and 4.71 mmHg for DBP |
| Our study | PCA-LS-SVM, PCA-SWR, PCA-ANN, PCA-ANFIS | BP reactivity to unsupported back | PCA-LS-SVM outperformed PCA-SWR, PCA-ANN, and PCA-ANFIS |

accuracy of BP measurements. However, validation of the computing models using a large database is indispensable to represent the true results outside the development population.

## 6 Conclusions

An unsupported back during BP measurement causes a significant rise in DBP, which may influence

the amount of treatment being given. The rise in DBP is greater in hypertensive individuals than that in normotensive ones. Furthermore, a performance comparison of PCA-SWR, PCA-ANN, PCA-ANFIS, and PCA-LS-SVM revealed the potential capability of the PCA-LS-SVM model in predicting BP reactivity to an unsupported back. The results of this study are highly encouraging and may provide valuable reference for researchers and engineers who apply hybrid models for the prediction of biological variables. The results are helpful in physicians' diagnosis, and they are also good for the prevention of hypertension in clinical medicine. Our future research is targeted at studying an ensemble system for combining outputs of multiple algorithms with more predictor variables.

## Compliance with ethics guidelines

All procedures followed were in accordance with the ethical standards of the responsible committee on human experimentation (institutional and national) and with the Helsinki Declaration of 1975, as revised in 2008 (5). Informed consent was obtained from all participants for being included in the study.

## References

Baba, R., Koketsu, M., Nagashima, M., *et al.*, 2007. Adolescent obesity adversely affects blood pressure and resting heart rate. *Circ. J.*, **71**(5):722-726. [doi:10.1253/circj.71.722]

Barbé, K., Kurylyak, Y., Lamonaca, F., 2014. Logistic ordinal regression for the calibration of oscillometric blood pressure monitors. *Biomed. Signal Process.*, **11**:89-96. [doi:10.1016/j.bspc.2014.01.012]

Basheer, I.A., Hajmeer, M., 2000. Artificial neural networks: fundamentals, computing, design, and application. *J. Microbiol. Method*s, **43**(1):3-31. [doi:10.1016/S0167-7012(00)00201-3]

British Hypertension Society, 1998. Blood Pressure Measurement (CD-ROM). BMJ Books, London, UK.

Card, D.H., Peterson, D.L., Matson, P.A., 1988. Prediction of leaf chemistry by the use of visible and near infrared reflectance spectroscopy. *Remote Sens. Environ.*, **26**(2):123-147. [doi:10.1016/0034-4257(88)90092-2]

Chiatti, C., Bustacchini, S., Furneri, G., *et al.*, 2012. The economic burden of inappropriate drug prescribing, lack of adherence and compliance, adverse drug events in older people. *Drug Saf.*, **35**(1):73-87. [doi:10.1007/BF03319105]

Cushman, W.C., Cooper, K.M., Horne, R.A., *et al.*, 1990. Effect of back support and stethoscope head on seated blood pressure determinations. *Am. J. Hypertens.*, **3**(3):240-241.

de Hoog, M., van Eijsden, M., Stronks, K., *et al.*, 2012. Association between body size and blood pressure in children from different ethnic origins. *Cardiovasc. Diabetol.*, **11**:136.1-136.10. [doi:10.1186/1475-2840-11-136]

Forouzanfar, M., Dajani, H.R., Groza, V.Z., *et al.*, 2011. Feature-based neural network approach for oscillometric blood pressure estimation. *IEEE Trans. Instrum. Meas.*, **60**(8):2786-2796. [doi:10.1109/TIM.2011.2123210]

Genc, S., 2011. Prediction of mean arterial blood pressure with linear stochastic models. Proc. IEEE Annual Int. Conf. on Engineering in Medicine and Biology Society, p.712-715. [doi:10.1109/IEMBS.2011.6090161]

Golino, H.F., Amaral, L.S.B., Duarte, S.F.P., *et al.*, 2014. Predicting increased blood pressure using machine learning. *J. Obes.*, **2014**:637635.1-637635.12. [doi:10.1155/2014/637635]

Gujarati, D.N., 1995. Basic Econometrics. McGraw-Hill, New York, USA.

Hagan, M.T., Menhaj, M.B., 1994. Training feedforward networks with the Marquardt algorithm. *IEEE Trans. Neur. Netw.*, **5**(6):989-993. [doi:10.1109/72.329697]

Haynes, R.B., Sackett, D.L., Taylor, D.W., *et al.*, 1978. Increased absenteeism from work after detection and labeling of hypertensive patients. *New Engl. J. Med.*, **299**(14):741-744. [doi:10.1056/NEJM197810052991403]

Huang, H.H., Xu, T., Yang, J., 2014. Comparing logistic regression, support vector machines, and permanental classification methods in predicting hypertension. *BMC Proc.*, **8**(Suppl. 1):S96.1-S96.5. [doi:10.1186/1753-6561-8-S1-S96]

Inoue, M., Minami, M., Yano, E., 2014. Body mass index, blood pressure, and glucose and lipid metabolism among permanent and fixed-term workers in the manufacturing industry: a cross-sectional study. *BMC Pub. Health*, **14**:207.1-207.8. [doi:10.1186/1471-2458-14-207]

Jang, J.S.R., 1993. ANFIS: adaptive-network-based fuzzy inference system. *IEEE Trans. Syst. Man Cybern.*, **23**(3):665-685. [doi:10.1109/21.256541]

Jolliffe, I.T., 2002. Principal Component Analysis. Springer-Verlag, New York, USA.

Kaiser, H.F., 1960. The application of electronic computers to factor analysis. *Educ. Psychol. Meas.*, **20**:141-151. [doi:10.1177/001316446002000116]

Khan, S.M.U., Manzoor, J.S., Lee, S.U.J., 2014. Predicting student blood pressure by support vector machine using Facebook. Proc. IEEE World Congress on Services, p.486-492. [doi:10.1109/SERVICES.2014.92]

Kolade, O.O., O'Moore-Sullivan, T.M., Stowasser, M., *et al.*, 2012. Arterial stiffness, central blood pressure and body size in health and disease. *Int. J. Obes.*, **36**(1):93-99. [doi:10.1038/ijo.2011.79]

Kurylyak, Y., Lamonaca, F., Grimaldi, D., 2013. A neural network-based method for continuous blood pressure estimation from a PPG signal. Proc. IEEE Int. Conf. on Instrumentation and Measurement Technology, p.280-283. [doi:10.1109/I2MTC.2013.6555424]

Lynn, S., Ringwood, J., Ragnoli, E., *et al.*, 2009. Virtual metrology for plasma etch using tool variables. Proc. IEEE/SEMI Advanced Semiconductor Manufacturing Conf., p.143-148. [doi:10.1109/ASMC.2009.5155972]

Monte-Moreno, E., 2011. Non-invasive estimate of blood glucose and blood pressure from a photoplethysmograph by means of machine learning techniques. *Artif. Intell. Med*., **53**(2):127-138. [doi:10.1016/j.artmed.2011.05.001]

Moser, D.C., Giuliano, I.C.B., Titski, A.C.K., *et al.*, 2013. Anthropometric measures and blood pressure in school children. *J. Pediatr*., **89**(3):243-249. [doi:10.1016/j.jped.2012.11.006]

Nauck, D., 1997. Neuro-Fuzzy Systems. John Wiley & Sons, Inc., New York, USA.

Noori, R., Khakpour, A., Omidvar, B., *et al.*, 2010. Comparison of ANN and principal component analysis—multivariate linear regression models for predicting the river flow based on developed discrepancy ratio statistics. *Expert Syst. Appl*., **37**(8):5856-5862. [doi:10.1016/j.cswa.2010.02.020]

O'Brien, E., Asmar, R., Beilin, L., *et al.*, 2003. European society of hypertension recommendations for conventional, ambulatory and home blood pressure measurement. *J. Hypertens*., **21**(5):821-848.

Pickering, T.G., Hall, J.E., Appel, L.J., *et al.*, 2005. Recommendations for blood pressure measurement in humans and experimental animals. Part 1: Blood pressure measurement in humans: a statement for professionals from the Subcommittee of Professional and Public Education of the American Heart Association Council on High Blood Pressure Research. *Hypertension*, **45**:142-161. [doi:10.1161/01.HYP.0000150859.47929.8e]

Schölkopf, B., Smola, A.J., 2002. Learning with Kernels. MIT Press, Cambridge, MA, USA.

Sharma, S., 1995. Applied Multivariate Techniques. John Wiley & Sons, Inc., Canada.

Smith, K.W., Sasaki, M.S., 1979. Decreasing multicollinearity: a method for models with multiplicative functions. *Sociol. Methods Res.*, **8**(1):35-56. [doi:10.1177/004912417900800102]

Suykens, J.A.K., Vandewalle, J., 1999. Least squares support vector machine classifiers. *Neur. Process. Lett*., **9**(3):293-300. [doi:10.1023/A:1018628609742]

Tobias, S., Carlson, J.E., 1969. Brief report: Bartlett's test of sphericity and chance findings in factor analysis. *Multivar. Behav. Res*., **4**(3):375-377. [doi:10.1207/s15327906mbr0403_8]

Williams, B., Brown, T., Onsman, A., 2010. Exploratory factor analysis: a five-step guide for novices. *Aust. J. Paramed*., **8**(3):1.1-1.13. [doi:10.1023/A:1011131521933]